

Available online at www.sciencedirect.com

jmr&t
Journal of Materials Research and Technology
www.jmrt.com.br



Original Article

Strengthening of stainless steel weldment by high temperature precipitation[☆]



Sergio Neves Monteiro*, Lucio Fabio Cassiano Nascimento, Édio Pereira Lima Jr.,
Fernanda Santos da Luz, Eduardo Sousa Lima, Fábio de Oliveira Braga

Military Institute of Engineering (IME), Materials Science Department, Rio de Janeiro, RJ, Brazil

ARTICLE INFO

Article history:

Received 31 May 2017

Accepted 5 September 2017

Available online 1 November 2017

Keywords:

Stainless steel

Weld

AISI 304

Precipitation hardening

ABSTRACT

The mechanical behavior and the strengthening mechanism of stainless steel welded joints at 600 °C have been investigated. The welds were composed of AISI 304 stainless steel, as base metal, and niobium containing AISI 347 stainless steel, as weld metal. The investigation was conducted by means of creep tests. The welded specimens were subjected to both high temperature (600 °C) and long periods (up to 2000h) under constant load, and both mechanical properties and microstructural changes in the material were monitored. It was found that the exposure of the material at 600 °C under load contributes to a strengthening effect on the weld. The phenomenon might be correlated with an accelerated process of second phase precipitation hardening.

© 2017 Brazilian Metallurgical, Materials and Mining Association. Published by Elsevier Editora Ltda. This is an open access article under the CC BY-NC-ND license (<http://creativecommons.org/licenses/by-nc-nd/4.0/>).

1. Introduction

Several mechanical components and structures that operate at high temperatures have been produced using austenitic stainless steels, due to its high resistance to hot oxidation and creep [1,2]. These systems are extensively fabricated using welding processes for strong and reliable joints [3–7]. Typical welded components and structures are found in petroleum refinery towers and fast nuclear reactors [8–11]. Welding electrodes made of stainless steel either contain low carbon or carbide formation alloy elements such as titanium (Ti) and niobium (Nb). This is a basic requirement to avoid a serious

corrosion problem, known as sensitization, associated with chromium carbide grain boundary precipitation.

The welding of a largely employed austenitic stainless steel, the AISI type 304, may use not only electrodes of low carbon AISI type 308, but also Ti containing AISI type 321 or Nb containing AISI type 347 [12]. In the particular case of high temperature application of components and structures made of 304 steel, the main problem is not the hot oxidation, but changes in mechanical properties due to phase and microstructural transformations. It was earlier observed [13] that the welding thermal effects originate different kinds of ferrite, with distinct sizes, in the austenitic matrix. For long times operating at high temperatures, not only ferrite

[☆] Paper was a contribution part of the 3rd Pan American Materials Congress, February 26th to March 2nd, 2017.

* Corresponding author.

E-mail: snevesmonteiro@gmail.com (S.N. Monteiro).

<http://dx.doi.org/10.1016/j.jmrt.2017.09.001>

2238-7854/© 2017 Brazilian Metallurgical, Materials and Mining Association. Published by Elsevier Editora Ltda. This is an open access article under the CC BY-NC-ND license (<http://creativecommons.org/licenses/by-nc-nd/4.0/>).

Table 1 – Chemical composition (wt%) of austenitic stainless steels used in the weldment.

AISI type	C	Cr	Ni	Mn	Si	Nb
304 (base)	0.060	18.3	8.4	1.77	0.52	–
347 (weld)	0.084	18.9	9.1	1.40	0.65	0.93

transformation, but also precipitation of new phases and morphological changes of these phases were detected [14].

A previous evaluation of the performance at 700 °C of the 304 steel welded using 347 filler, reported by White and Le May [15], revealed a tendency of decreasing the mechanical strength with treating time. Indeed, after a brief period of strengthening in the fusion zone (FZ), carbide precipitation would reduce the strength of the joint, acting mainly in the heat affected zone (HAZ). By contrast, preliminary results at 600 °C [16,17] indicated strengthening of both the FZ and HAZ for the whole component operation life. This particular temperature, 600 °C, corresponds to the highest operation temperature required for 304 steel welded components. In those preliminary works, static mechanical properties were obtained for the 304/347 welds, at room temperature, after heat treatments at 600 °C. However, the high temperature structural changes under load are probably distinct from those static conditions, and so, creep tests might be a more adequate methodology for this evaluation.

Therefore, the objective of the present work is to evaluate the creep behavior of 304/347 welded joints at the temperature of 600 °C.

2. Materials and methods

The chemical compositions of the AISI 304 austenitic stainless steel rolled plate, supplied by Villares, Brazil, and the AISI 347 steel electrodes are presented in Table 1. The grain size of the as-received 304 steel plate was 75 μm.

Butt weld was performed according to procedures presented elsewhere [17]. Standard ASTM [18] round specimens with 6 mm of gage diameter and 38 mm of gage length were machined from different parts of the weldment. The series of specimens corresponding to position and length direction were identified as following:

- I – base metal along the plate rolling direction.
- SL – weld metal in the longitudinal direction.
- ST – weld metal in the transversal direction.
- J – specimens cut across the base metal/weld metal/base metal.

Creep tests were conducted at 600 °C in a tubular furnace of a WPM equipment, from Germany. Metallographic sections of tested specimens were polished with emery paper and diamond paste before etch with oxalic acid. Microstructure was observed in a Neophot optical microscopy.

3. Results and discussion

Typical creep curves are shown in Fig. 1, for specimens of the four distinct series: I, SL, ST and J. As illustrated, some tests

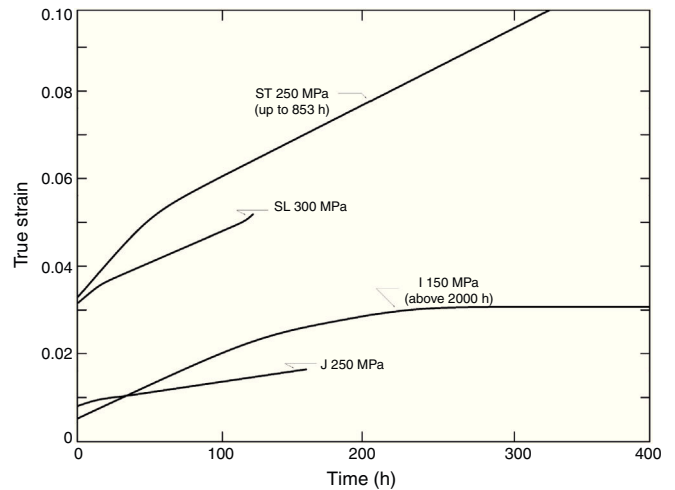


Fig. 1 – Typical creep curves for specimens associated with distinct positions and directions in the 304/347 steel weldment.

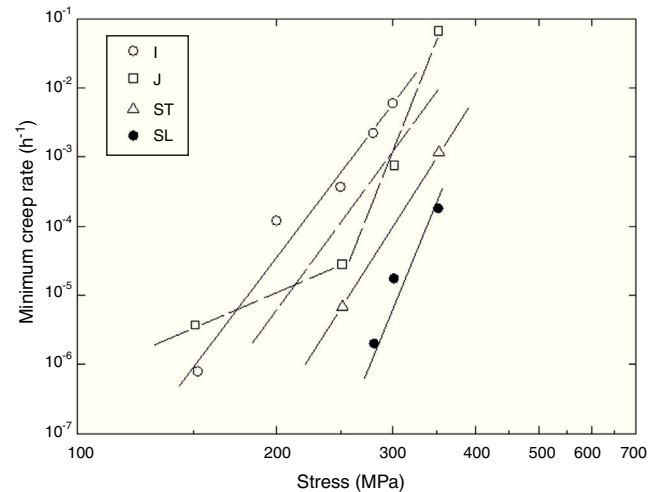


Fig. 2 – Variation of creep rate with stress for specimens associated with distinct positions and directions in the 304/347 steel weldment.

of the I series were stopped over 2000 h. In fact, I series corresponds to the base 304 steel, but did not include the weld metal 347 steel, responsible for the investigated thermal effects.

From curves such as those shown in Fig. 1, the minimum creep rate, $\dot{\epsilon} = d\epsilon/dt$, associated with the slope of stage II of creep [18], was calculated and plotted against the applied constant creep stress. Fig. 2 shows in a double log scale the variation of the creep rate with corresponding stress.

Excluding the J series, single straight lines were adjusted to corresponding points of series I, ST and SL. This indicates that a characteristic power law (Eqs. (1) and (2)) [18] holds between σ and $\dot{\epsilon}$.

$$\dot{\epsilon}_m = k \cdot \sigma^n \quad (1)$$

Table 2 – Exponent for the creep power law for specimen series associated with distinct positions and directions in the 304/347 steel weldment.

Specimen series	I	J	ST	SL
Value of n	12	4–25	19	19

or

$$\log \dot{\epsilon}_m = \log k + n \cdot \log \sigma \quad (2)$$

The points corresponding to J series in Fig. 2 apparently exhibit two different linear adjustments, i.e. a double- n behavior. The values of n obtained from Eqs. (1) and (2) are presented in Table 2.

The results in Fig. 2 and Table 2 indicate that at 600 °C the weld metal in both longitudinal (SL) and transversal (ST) directions display higher creep resistance than the base metal (I). Indeed SL and ST specimens possess lower creep rate than those from I series, Fig. 2, for the same level of stress. This phenomenon might be associated with carbide precipitation in the weld metal, such as the NbC [16], that acts as barriers to dislocations, leading to lower creep rates. It is known that the 347 stainless steel (weld metal) is basically the 304 SS with niobium added (Table 1). The niobium is a stabilizing element commonly added to reduce the sensitization of the steel and to strengthen the structures [2]. The Nb has higher chemical affinity with the carbon in comparison to the chromium, promoting a fine intergranular precipitation of niobium carbides, which inhibits the chromium precipitate [16,19]. The removal of chromium from the steel matrix, due to the formation of their carbides, decreases the passive film, weakening the weld joint. This does not conflict with White and Le May [15] findings, since there is no influence of the HAZ in the SL and ST series. This region (HAZ) was found to be negatively affected by the new phases precipitation, maybe because other carbide (such as the Cr₂₃C₆) or σ phase are being formed for a long time exposure in high temperature, causing the embrittlement.

Moreover, the value $n = 19$ for SL and ST are higher than that $n = 12$ for I series (Table 2), and this represents a higher strain rate sensitivity of the weld metal with the increasing stress.

As for the J series, the minimum creep rate is intermediary when compared to the I series and the weld metals series (SL and ST), for the same applied stress. This might be a consequence of the combination of creep mechanisms acting on the FZ and HAZ. The two slopes $n = 4$ and $n = 25$, Fig. 2 and Table 2, are also an indicative of this behavior, which reveals that for relatively short time creep, under higher stress, the highest value of n could be associated with a strengthening effect. Several studies have indicated the predominance of dislocation glide for high stresses [18]. As shown in Fig. 2, for a minimum creep rate $\dot{\epsilon} > 10^{-4}$, the power law increases from 4 to 25. This might be associated with the replacement of dislocation climb by dislocation glide, which is no longer controlled by diffusion at high stresses [18,20]. For Nassour and co-workers [21], at lower stresses, the deformation is associated with grain-boundary sliding or diffusional creep mechanism (as in dislocation climb), and at high stresses, with dislocation controlled mechanism.

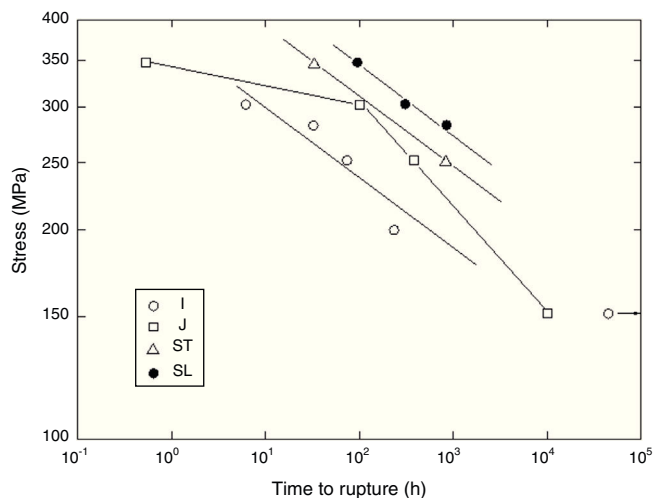


Fig. 3 – Variation of the creep stress with time to rupture for specimens associated with distinct positions and directions in the 304/347 steel weldment.

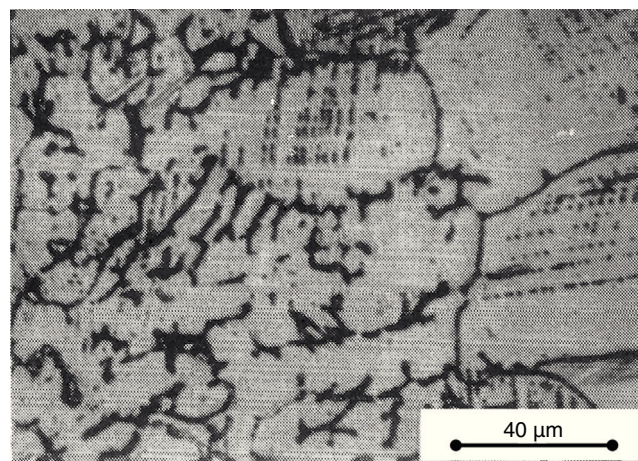


Fig. 4 – Optical micrograph of the transition from 347 weld metal (left region) to the 304 base metal (right region).

Another relevant creep parameter is the rupture time (t_r) [18]. Fig. 3 shows, in double log scale, the relation of the creep stress with time to rupture, for the distinct specimens in I, J, ST and SL series. Again, one should notice that, except for J series, linear adjustments might represent the behavior of I, ST and SL series. In the case of J specimens, two linear branches with different slopes could be observed. By comparing the slopes, it is predicted that both series comprising weld metal, ST and SL would have a longer time to rupture at extrapolated lower stresses. In other words, in normal operational conditions of relatively lower stresses at 600 °C, the base metal (304 steel plate) would fail before the 347 steel weld metal. However, from the results in Fig. 3, it is not clear whether the combined region base/metal/base metals, series J, might fail even before the base metal. This could be a consequence of the carbide precipitation [15].

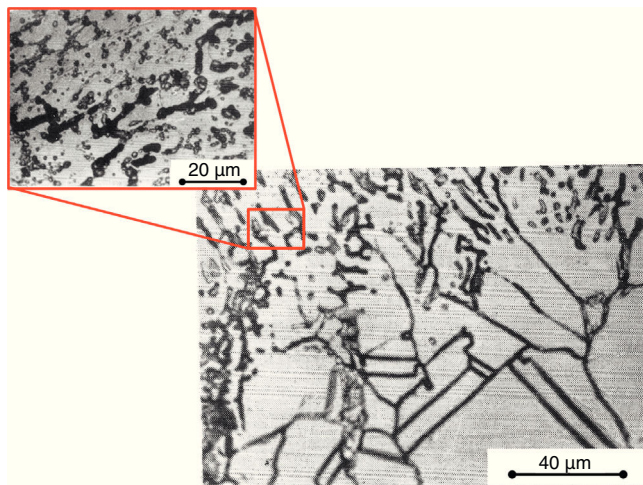


Fig. 5 – Weldment transition zone after creep at 600 °C and 250 MPa for 300 h.

Fig. 4 shows the typical microstructure of the transition region from the FZ (in the left) to the base metal (in the right), before the creep tests. Only dendrite formation can be seen in the FZ, and there is no evidence of carbide precipitation. Fig. 5 shows a similar image, with typical microstructure of the transition region in the J specimens, after the 600 °C creep tests, treated under 250 MPa load for 300 h. In this figure, profuse carbide precipitation occurred in the weld metal, evidenced as small round precipitates in the higher magnification insert. In addition to carbide precipitation, which is common in the 347 steel weld at 600 °C, sigma phase would also be expected, due to the long time exposure of an austenitic stainless steel at high temperature [16,17]. The larger dark grain boundary precipitates might represent this feature. The two distinct precipitates evidenced in the micrographs, attributed to carbide precipitation and sigma phase transformation, might be responsible for the strengthening effect.

4. Conclusions

- Creep tests performed at 600 °C under different constant stresses in distinct parts of a weldment comprising AISI type 304 austenitic stainless steel as base metal and niobium containing AISI type 347 austenitic stainless steel as weld material revealed an strengthening effect at the weld.
- Lower creep rate and longer rupture time were associated with this strengthening effect. Creep specimens combining both base and weld metals displayed a significantly higher value of the power law exponent n for relatively short time creep.
- Metallographic evidence showed carbide precipitation and sigma phase deformation occurring at the weld metal. This was associated with the creep strengthening of the weldment.

Conflicts of interest

The authors declare no conflicts of interest.

Acknowledgements

The authors of the present work wish to thank the Brazilian supporting agencies CAPES, CNPq and FAPERJ for the funding and scholarships.

REFERENCES

- [1] Marshal P. *Austenitic stainless steels microstructure and properties*. London: Elsevier; 1984.
- [2] International ASM. *Handbook. Properties and selections: irons steels and high-performance alloys, vol. 1, 10th ed.* Materials Park, OH: ASM International; 2010.
- [3] Mazancova E, Ostroushko D, Saksli K, Nieslony A. Joint hydrogen susceptibility of 304 SS welded with titanium. *Arch Metall Mater* 2014;59:1605–10.
- [4] Bai T, Guan KS. Evaluation of stress corrosion cracking susceptibility of nanocrystallized stainless steel 304L welded joint by small punch test. *Mater Des* 2013;52:849–60.
- [5] Younes CM, Steele AM, Nicholson JA, Barnett CJ. Influence of hydrogen content on the tensile properties and fracture of austenitic stainless steel welds. *Int J Hydrog Energy* 2013;38:4864–76.
- [6] Srinivasan G, Divya M, Albert SK, Badhuri AK, Klenk A, Achar DRG. Study of hot cracking behavior on nitrogen-enhanced austenitic stainless steels using Vareststraint and hot ductility tests. *Weld World* 2010;54:R322–32.
- [7] Naffakh H, Shamanian M, Ashrafzadeh F. Dissimilar welding of AISI 310 austenitic stainless steel to nickel-based alloy Inconel 657. *J Mater Proc Technol* 2009;209:3628–39.
- [8] Veternikova JS, Degmova J, Pekarcikova M, Simko F, Petriska M, Skarba M, et al. Thermal stability study for candidate stainless steel of GEN IV reactors. *Appl Surf Sci* 2016;387:965–70.
- [9] Badhuri AK, Laha K, Ganesan V, Sakthivel T, Nandagopal M, Reddy GVP, et al. Advanced materials for structural components of Indian sodium-cooled fast reactors. *Int J Press Vessels Pip* 2016;139:123–36.
- [10] Nakae N, Ozawa T, Ohta H, Ogata T, Sekimoto H. An approach for evaluating the integrity of fuel applied in innovative nuclear energy systems. *J Nucl Mater* 2014;446:1–9.
- [11] Parthasarathi NL, Borah U, Albert SK. Effect of temperature on sliding wear of AISI 316 L(N) stainless steel – analysis of measured wear and surface roughness of wear tracks. *Mater Des* 2013;51:676–82.
- [12] International ASM. *Handbook. Welding, brazing and soldering, vol. 6, 10th ed.* Materials Park, OH: ASM International; 2011.
- [13] De Long WT. Ferrite in austenitic stainless steel weld metal. *Weld J Res Suppl* 1974;53:273–86.
- [14] Spruiell JE, Fett W, Lundin C. Ferrite stability at elevated temperature in austenitic stainless steel weld metal. *Weld J Res Suppl* 1977;56:289–90.
- [15] White WE, Le May I. Metallographic observations on the formation and occurrence of ferrite, sigma phase and carbides in austenitic stainless steels. Part III. Electron microscopy studies. *Metallography* 1972;5:333–45.

-
- [16] Pope AM, Silveira TL, Monteiro SN. Mechanical strengthening by 600 °C precipitation AISI 304/347 welded joints. *Metal ABM* 1979;35:103–7 [in Portuguese].
- [17] Pope AM, Silveira TL, Monteiro SN. Rupture under constant load at 600 °C of AISI 304/347 welded joints. *Metal ABM* 1980;36:155–60 [in Portuguese].
- [18] Meyers MA, Chawla KK. *Mechanical behavior of materials*. 2nd ed. Cambridge, UK: Cambridge University Press; 2009.
- [19] Guan K, Xu X, Xu H, Wang Z. Effect of aging at 700 °C on precipitation and toughness of AISI321 and AISI 347 austenitic stainless steel welds. *Nucl Eng Des* 2005;235(23):2485–94.
- [20] Kestenbach HJ, Krause W, Silveira TL. Creep of 316 stainless steel under high stresses. *Acta Met* 1978;26:661–70.
- [21] Nassour A, Bose WW, Spinelli D. Creep properties of austenitic stainless-steel weld metals. *J Mater Eng Perform* 2001;10:693–8.